

TiO₂–CeO₂ Ceramic Nanocomposites: Synthesis, Characterization, and Dielectric Characteristics at Low Titania Concentrations

Dr. Shashwati Vijay Pradhan^{1*} Meenal Pathak²

¹ Assistant Professor, R. D. National College, Bandra, West-Mumbai

² Lecturer in Jiwaji University, Gwalior

Abstract – TiO₂(x)–CeO₂ (1–x) TiO₂ and CeO₂ nano-particles produced by the polymeric citrate precursor technique were used for low TiO₂ composition of 5%, 10%, 15% and 20%. The characteristics of these nanocompositions were the use of powder x-ray diffraction, electron microscope transmission, electron microscopy scan, x-rays energy dispersion analysis and BET surface area study. The special surface area of the preparations for nanocomposites within the range of 239–288 g⁻¹ was shown in BET tests. For all TiO₂ Titanium-Ceria nanocomposites the lowest average particle sizes of 30 nm and the largest surface area of 288 m² is the nanos generated. Dielectric characteristics are accessed via frequency and temperature. TiO₂(x)–CeO₂ (1–x) Dielectric constant at room temperature at 500 kHz was $x = 0.20$.

Keywords – Polymeric Citrate Precursor Method; Nanocomposites; Dielectric Properties.

-----X-----

INTRODUCTION

The global energy demand for electronic devices is increasing every day as the world's population continues to rise. The portability of such devices is an important characteristic for easy and efficient operation. Consequently, efforts have been continuously undertaken to miniaturise the components required to construct these devices that require the synthesis of new materials which are highly dielectrical, low dielectric and high thermal stability[1]. The nanosized titanium (TiO₂) has received great attention from material scientists due to its common availability, non-toxicity, excellent thermal strength and strong dielectric constancy. Although TiO₂ is known to be found mainly in crystallographic anatases, rutiles and brookites, the TiO₂ polymorphes are more prevalent in both anatase and rutile forms. Rutile forms were stable in comparison to the anatase form of TiO₂ at higher temperatures. The TiO₂ nanocrystalline anatase is used for water purification to eliminate organic pollutants[3], to improve its optometric characteristics in light-emitting diodes and as antibacterial agent in bioscience[2]. Usually, as compared to the anatase shape, the rutile shape shows a better dielectric constant value and is thus employed in low-temperature co-fired ceramics [3]. The crystallographic structure of the two shapes is different for the rutile high dielectric constant. Anataasis consists of a four-edge framework of distorted TiO₆ octahedral units, whereas the rutile

form of TiO₂ is linked to trans-edge octahedral TiO₆ chains by shared corners. The literature indicated a dielectric constant of 80 for TiO₂ rutile nanoparticles[4]. Wypych et colleagues have produced TiO₂ nanosized for its dielectric characterisation using several chemical techniques at varying temperatures of synthesis.

The investigation reveals a substantial influence on the dielectric properties of TiO₂ due to the size of nanoparticles, relative density and synthesis temperature. In both anatase and rutile structure, TiO₂ nanoparticles, produced by sol-gel technique at the temperature of 600 and 850 Celsius were stable. Dielectric constants at the room temperature were obtained at frequency 18.9 (for anatase) and at frequency 63.7 (for rutile). TiO₂ nanoparticles were produced in 900 umbilical pechinis (anatase and rutile) utilising a 900 daC technique for which a dielectric dielectric temperature constant of 17 was present due to a phase of anatase[5]. Marinel et al. observed a consistent dielectric value of around 100 nanoparticles of TiO₂, sintered at 1000–1300 lib. Temperature. The fluorite structure of Cubic CeO₂ is similar. The fluorite structure of the CeO₂ is stable throughout a broad range of dielectric temperatures ($k = 23$). It is thus seen as a very attractive option in terms of dielectric gate in the semiconductor for metal oxides and memory device for future generation devices.

Titania based nanocomposites as a photocatalyst

A semiconductor material with outstanding dielectric, electrical and physical-chemicals surface characteristics, titanium dioxide is a titanium compound. In the presence of UV light it exhibits good photocatalytic efficiency. The intriguing grey matter of scientists has prompted Titania to focus on how to use the whole spectrum of visible light. The obstacle facing them was a bigger 3 eV band gap and more, thus attempts were made to add additional material to Titania. This paper examines the current progress on the synthesis and photocatalytic effectiveness of various titanium-based nanocomposites in numerous applications such as dyes, other water pollutants, microorganisms and metals, etc. There is also a short description of the photocatalytic process and structural characteristics of TiO₂. Various historical and contemporary methods to photocatalytic photocomposites based on Titania have been examined. The kinetics of photo-corrosion and thermodynamical components of photo-corrosion of various composites created by the various groups across the globe are proposed in order to make commercial use of nano-composites based on Titania.

Interfacial and Surface Structures of TiO₂-CeO₂ Mixed Oxides

The interfacial and surface structures of CeO₂-TiO₂ sol-gel mixed oxides, X-rays (XRD), BET surface area measurement, X-rays (XAs), HRTEM (High-Resolution Microscope Transmission Electron Electron) and selection of the chemical orange were thoroughly investigated. Methyl orange is the most commonly used method of transmission. TiO₂ and CeO₂ are mixed oxides in CeO₂-TiO₂ respectively in anatase phase and cubic fluorite phase. The mixed oxides have significantly larger surfaces than the single oxides and both mesopores and micropores. The results of XAS show that Ce atoms form a Ce-O-Ti interface in mixed oxides as cubic (CeO₈) polyhedrons. The cubic fluorite CeO₂ crystallites progressively form with the increasing Ce/TiO₂ weight ratio. TiO₂ anatase produces ultrafine particulate matter in mixed oxides which, due to the presence of CeO₂, have a local structure. The findings of the HRTEM indicate the Ce content for the exposed mixed oxide surfaces. Meteorange chemisorptions findings which were shown to adsorb deeply on ceO₂, but less in TiO₂, show that the adsorption capacity of ceO₂ to methyl orange in mixed oxides was much lower than that of pure ceO₂. Our results illustrate the way in which complex mixed oxides, which are of considerable relevance in understanding their characteristics, are characterized interfacial and surface structures.

Potentials and opportunities in nanocomposites

Let's look at the potential of these systems and the overall prospects before we get into depth on the

treatment, structure, characteristics and applications of the three types of nanocomposites. Ceramics have strong resistance to wear and have great thermal and chemical resilience. They're fragile, though. The poor hardness of ceramics in that context has remained a hindrance to its further application in industry. The ceramic-matrix nanocomposites received attention in order to overcome this restriction, largely because of considerable improvement in the mechanical characteristics. An enhancement of fracture toughness may be due, for example, to the incorporation of energy dissipating components such as whisker, fibre, platlets or particles into the matrix. The reinforcements deflect the fracture and/or supply bridging components that prevent the crack from further opening. Furthermore, in combination with the expansion in volume caused by the stress field of a propagating crack, the included phase underwent a phase change, contribute to the toughing and strengthening procedure, even in nanocomposites³⁶. The pioneering work of Niihara has highlighted the promise of the ceramic matrix nanocomposites (CMNC), primarily of Al₂O₃/SiC. Most investigations noted thus far verified that the Al₂O₃ matrix has been strengthened after adding a small volume of SiC particles of appropriate size (~ 10 percent) and the consequent hot pressure to the mixture. Some research have described this toughing mechanism on the basis of the nano sized reinforcements' cracking role³⁹. The integration of high strength nano fibers into ceramic matrices has therefore enabled for the creation, in comparison to abrupt failures of ceramic materials, of advanced nanocomposites with high strength and improved failure characteristics.

The phase is transitioned to the volume expansion begun by a propagating fracture stress area, which helps even in nanocomposites toughen and enhance processes. The pioneering work of Niihara has demonstrated the potential of ceramic matrix of nanocomposites (CMNC), especially the Al₂O₃/SiC system. The majority of investigations reported in recent years verified that the Al₂O₃ matrix is significantly strengthened after adding a little (~10 percent) volume of SiC particles of the appropriate size and heat pressure to the resultant mix. Some research has described this tightening mechanism on the basis of the nano sized reinforcements' cracking action. As a result, the integration of high resistance nano fibers into ceramic matrix allows for the creation in comparison with abrupt failures of ceramic materials of advanced nano composites with high resistance and better failure properties.

OBJECTIVES OF THE STUDY

- Pure TiO₂ and CeO₂ nanoparticles were synthesized by using polymeric citrate precursor.

- The synthesis of $\text{TiO}_2(x)\text{-CeO}_2 (1-x)$ nanocomposites by using prepared TiO_2 and CeO_2 nanoparticles in suitable amounts.
- The dielectric characteristics of the nanocomposites were studied as a function of frequency and temperature.

RESEARCH METHODOLOGY

MATERIAL AND METHODS

Chemicals required

Citric acid (SRL, 99.5%), ethyleneglycol (SDFCL, 99%), titanium isopropoxy (SigmaAldrich, 97%) and cerium heptahydrate will be utilised in the chemical products (CDH, 99 percent). Without additional purification, all compounds will be utilised. The water used in the production of nanocomposites is twofold distilling.

Synthesis of precursor nanoparticles

A constantly swirling beaker containing 1,4 ml of ethylene glycol has also been added 21 grammes and 14 milligrammes of dried citric acid. In the beaker with ethylene glycol, a clear solution will be added to the beaker with 23.6 ml double distilled water and mixed for 30 minutes. In the inert chemical set-up, a continuous purging of nitrogen gas will be devised to add 0.74 ml of titanium isopropoxide to the initial solution to ensure molar ratio of 10:40:1 will be applied to ethylene glycol, citric acid and titanium isopropoxide. At first, white precipitates will be produced due to the production of titanium hydroxide, dissolved under nitrogen environment by continuous agitation. The ringing will be allowed to create a clear transparent solution for 3 hours at room temperature. For 2 hours, the solution will be added to 55 ± 5 daC to enhance the solution viscosity. The viscous solution will be placed into the furnace and continuously heated for 20 h at a temperature of 135°C , so that the solvent excess could be eliminated as vapours and the polymerizing reaction accelerated. At 300 p.c. (2 h) the polymer gel will be further processed to achieve the black charred product pulverized to the fine powder (precursor). The black fine powder will be further heated to produce TiO_2 anatase for a 20 hour period in a microprocessor-controlled hoist furnace at 500 ppc.

25 ml 0.1 M $\text{CeCl}_3 \cdot 7\text{H}_2\text{O}$ will be added in order to make CeO_2 nanoparticles to the 1,4 ml beaker with continual stirrings of ethylene glycol. Sluggish additions of 21 grammes and 14 milligrammes of citric acid will be achieved, resulting in a milky tint that rapidly vanished into a clear solution and agitated for three hours at room temperature. The remainder of the method will be the same as the TiO_2 synthesis.

Synthesis of nanocomposites

$\text{TiO}_2\text{-CeO}_2$ Mixing TiO_2 with CeO_2 with 5, 10, 15 and 20 percent w/w of TiO_2 , followed by the correct 1 hr grinding, produced nanocomposites. To improve nano-powder adherence, a few drops (5% PVA), which will be allowed to cure for 1 hour at 100 psiC, will be added to the solution. The powders subsequently will be pelleted and sintered for composite measurements by 1000 bar C for 10 hours. Two nanocomposite pellets have been produced. One pellet will be utilized to test dielectric properties, while the others will be grinded for 1 h to produce fine powder to carry out other characteristics.

Characterization

The sophisticated X-ray diffractometer Bruker D8 will be utilised in the investigations of XRD employing Ni-filtered $\text{CuK } \alpha$ wave-long radiations ($\lambda = 1.5416 \text{ \AA}$). Patterns will be captured for 2 channels in the range 20–80 channels and for 1 s step duration and 0.05 channels step size. By applying the stripping method for $\text{K}\alpha_2$ reflections, the grid parameters will be determined. The morphology of the FEI SEM samples as prepared has been analysed using SEM investigations (model: Nova Nano SEM 450, Hillsboro, OR). For samples prepared by grinding sintered pellets at different magnifications, SEM pictures will be acquired in powder shape. In order to determine the composition of the Nanocomposites, EDAX conducted an elemental analysis using 127 eV Bruker EDX detector. TEM observations using the FEI Technai G220 TEM with an accelerating voltage of 200 kV have been investigated. A limited number of samples in fine powder form will be collected for the fabrication of TEM specimens to be sunken in 100% ethanol. Half an hour will be done with the sonication. A drop of the material will be placed using a micropipette (100 μl) on a carbon-coated copper grid and dried up in the centime.

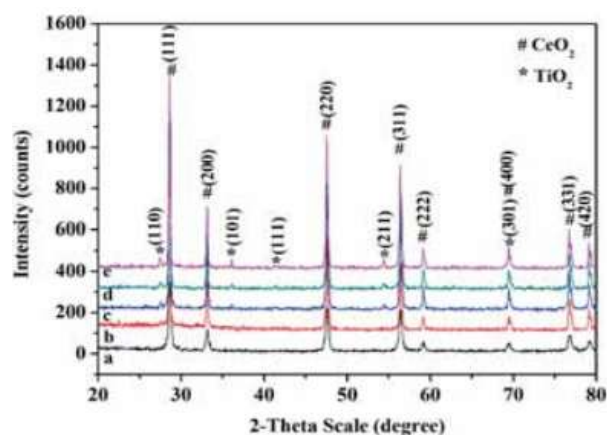


Figure 1: The ceria(a) and titanium-ceria nanocomposite X-ray diffraction patterns for (b) $x = 0.05$, (c) $x = 0.10$, (d) $x = 0.15$ and (e) $x = 0.20$

Dielectric properties of the synthesized HFLCR metre of nano-composites have been reported (model: 6505P; Make: Wayne Kerr, UK). The diameter and thickness of the pellets had to be calculated and the area of the pellets estimated in order to examine dielectrical characteristics of nanocomposites utilizing condenser values before dielectric tests.

RESULTS AND DISCUSSION

After the heating of 1000 to C pellets for 10 h, XRD investigations of the TiO₂(x)-CeO₂ (1-x) nano-composites (x = 0.05, 0.10, 0.15 and 0.20) will be performed. The PXRD patterns have been successfully indexed to the CeO₂ (JCPDS No. 81-0792) (Fm3-m(225) and a = 5.412 Å) space group, and the tetragonal (rutile) structure (JCPDS No. 83-2242) (P42/mnm (136) space group), a = 4.59 and b = 2.96 Å structure (figure 1). All samples will be extremely crystalline and biphasic in character. The XRD analyses show clearly that there is no peak but CeO₂ and TiO₂, which demonstrate that TiO₂-CeO₂ nanocomposites are the previously produced materials. The presence in the two-party peaks of (110), (101), (211) and (301) is consistent with the existence of rutile TiO₂ in 2 PV values of 27.5, 36, 41, 54.3 and 69.5 SE. In conclusion, the PXRD results indicated a rise in the peak intensity of the rutile TiO₂ phase in host CeO₂ matrix with increasing TiO₂ content.

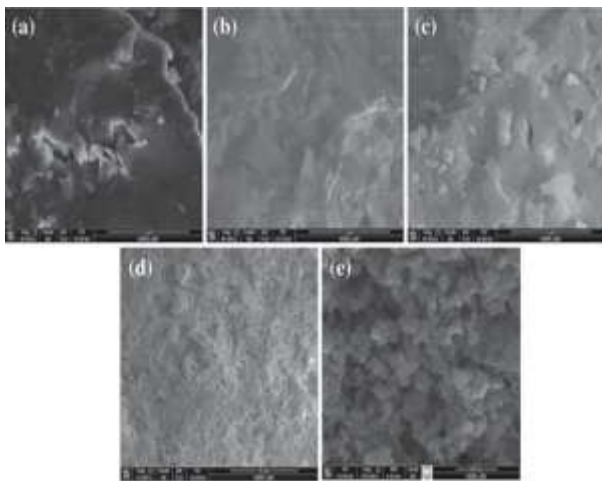


Figure 2: SEM nanocomposite titanium-cerium micrographs (a) x = 0.05, (b) x = 0.10, (c) x = 0.15, (d) x = 0.20 and (e) pure ceria nanoparticles.

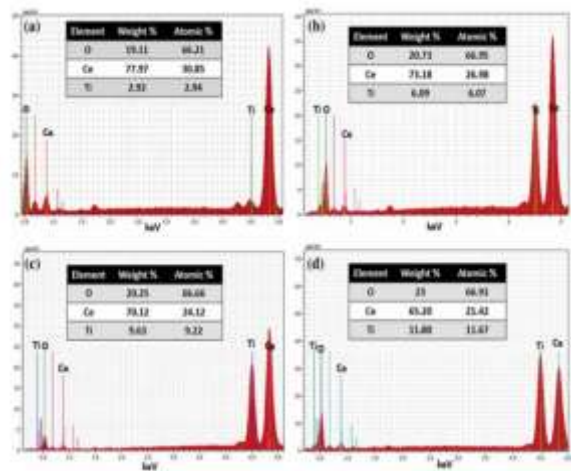


Figure 3: EDAX spectra of titania-ceria nanocomposites for (a) x = 0.05, (b) x = 0.10, (c) x = 0.15 and (d) x = 0.20.

TiO₂(x)-CeO₂ (1-x) nano-composite morphology and texture will be examined using SEM investigations. The SEM pictures clearly illustrate the biphasic morphology, where nanoparticles TiO₂ could be clearly visible on a rough surface of CeO₂. In the SEM pictures of pure CeO₂, the nanoparticles will be agglomerated with almost spherical forms, as seen in figure 2e. This can be observed in Figure 2d with increasing titanium content percentage, higher density of nanocomposites and hence dense surface. The EDAX experiments demonstrate that the precursor nanoparticles' loaded compositions correspond very well with the predicted nanocomposite composition displayed in Figure 3a-d. The study of XRD and EDAX confirms that nanocomposites form TiO₂-CeO₂.

Surface area investigations of produced nanocomposites will be performed utilizing the multi-point BET equation in the P/P₀ range of 0.05-0.35. The BET plots indicated that 239-288 g⁻¹ will be detected on the specified surface area for the nanocomposites. Pure CeO₂ has a specific surface area of 258 m² g⁻¹. The surface area has increased, with the percentage of TiO₂ in nanocomposites increasing. The particle size will be also calculated with the DBET = 6000/(S) calculation. DBET represents in this equation an average nm particle size, the theoretically μg/m³ and the Sw is the specific surface of m² g⁻¹ in this equation. For nanocomposites with 5, 10, 15 and 20% TiO₂, the particulate size used for the aforementioned BET tests will be 7.4, 7.1, 6.9 and 5.9 nm. The values of kernel sizes will be less than TEM values, since for the spherical particles with a smooth surface theory applies BET sizes. The BET size values are therefore qualitatively valid, but the spherical geometry and smooth surface of the particles are absent from the present research. The form factor for nanoparticles will be therefore examined.

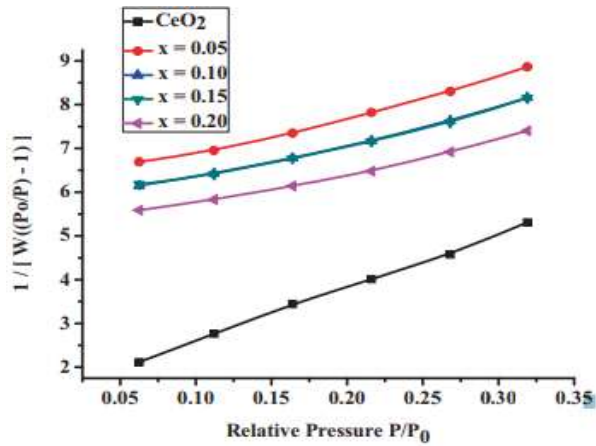
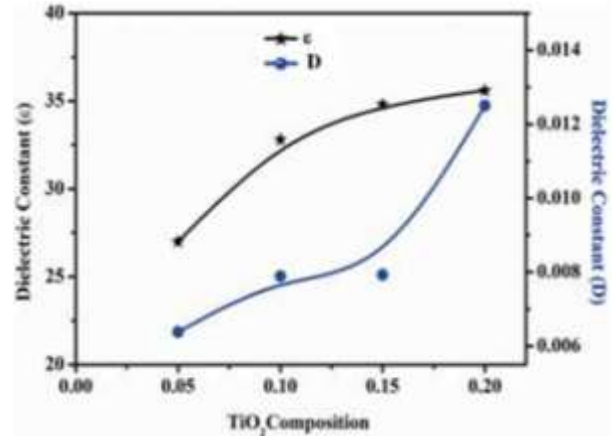


Figure 4: BET surface area plots of titania–ceria nanocomposites for (a) $x = 0.05$, (b) $x = 0.10$, (c) $x = 0.15$, (d) $x = 0.20$ and (e) pure ceria nanoparticles.

Dielectric constant and dielectric loss of produced nanocomposites will be also examined as a temperature function at 500 kHz. For all ceramic nanocomposites ($\text{TiO}_2(x)\text{-CeO}_2(1-x)$ ($x=0.05, 0.10, 0.15$ and 0.20), the experimental dielectric constancy and dielectric loss values will be found to be steady for 250 gr. and an increase in temperature will be seen afterwards. Dielectric constant increases over 250 degrees Celsius can be caused by the increasing pooling with the applied field, which leads to the interaction between the field and dielectric polarity. The dielectric properties of $\text{TiO}_2(x)\text{-CeO}_2(1-x)$ nanocomposites at a value of 200C will be 27.3, 0.025 (for $x= 0.05$), 33, 0.033 (for $x=0.10$), 34.7, 0.041 (for $x = 0.15$) and 35.4, 0.042 (for $x = 0.20$). It will be observed that the dielectric constant increases with a higher TiO_2 content in Nanocomposites $\text{TiO}_2\text{-CeO}_2$, which might be linked to a high dielectric consistency of nanoparticles TiO_2 .

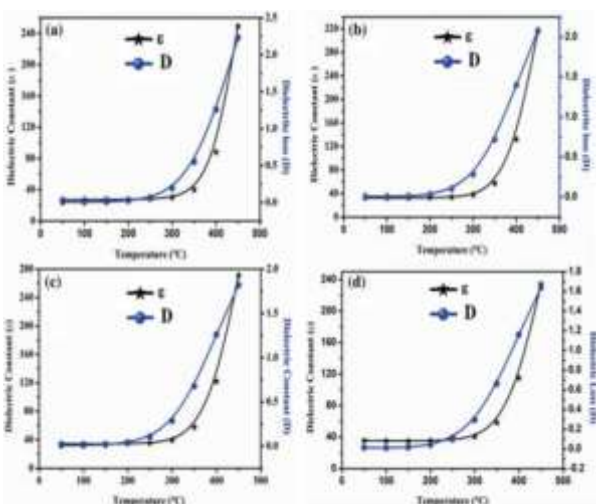


CONCLUSION

Ceramic nanocomposites of $\text{TiO}_2(x)\text{-CeO}_2(1-x)$ ($x = 0.05, 0.10, 0.15$ and 0.20) Appropriate quantity of nanoparticles TiO_2 and CeO_2 that have been produced through the polymeric citrate precursor method have successfully been synthesized. Biphasic, reasonable agglomeration and rough surfaces will be created nanocomposites. Along with certain spherical particles, the nanocomposites were almost hexagonal. The size of the particles decreases from 46 to 30 nm when the concentration of titanium is increased from 5 to 20 percent. As a result, with an increase in titanium percentage composition the specific surface area increases substantially. The nanocomposites have strong dielectric characteristics with a frequency fluctuation of 20 to 500 kHz and temperature variation up to 250 pp. The dielectric constant was observed to rise owing to strong dielectric properties of titanium in the percentage of TiO_2 in $\text{TiO}_2\text{-CeO}_2$ nanocomposites.

REFERENCES

1. Wilk G. D., Wallace R. M. and Anthony J. M. (2001). J. Appl. Phys. 89, pp. 5243
2. Zhang H. and Banfield J. F. (2002). Chem. Mater. 14, pp. 4145
3. Tayade R. J., Surolia P. K., Kulkarni R. G. and Jasra R. V. (2007). Sci. Technol. Adv. Mater. 8, pp. 455.
4. Al-Asbahi B. A., Jumali M. H. H., Yap C. C. and Salleh M. M. (2013). J. Nanomater. 561534, pp. 1.
5. Ahmad R., Mohsin M., Ahmad T. and Sardar M. (2015). J. Hazard. Mater. 283, pp. 171
6. Pang L. X., Wang H., Zhou D. and Yao X. (2010). J. Mater. Sci. 21, pp. 1285
7. Wypych A., Bobowska I., Tracz M., Opasinska A., Kadlubowski S., Krzywani-



- Kaliszewska A., et. al. (2014). *J. Nanomater.* 124814 1
8. Marinel S., Choi D. H., Heuguet R., Agrawal D. and Lanagan M. (2013). *Ceram. Int.* 39 299
 9. Chiu F. C. and Lai C. M. (2010). *J. Phys. D: Appl. Phys.* 43 (075104)
 10. Tarnuzzer R. W., Colon J., Patil S. and Seal S. (2005). *Nano Lett.* 5, pp. 2573.
 11. Phokha S., Pinitsoontorn S., Chirawatkul P., Poo-Arporn Y. and Maensiri S. (2012). *Nanoscale Res. Lett.* 7, pp. 1.
 12. Nilchi A., Darzi S. J., Mahjoub A. R. and Garmarodi S. R. (2010). *Colloids Surf. A: Physicochem. Eng. Aspects* 361, pp. 25.
 13. Shanker V., Ahmad T. and Ganguli A. K. (2006). *J. Mater. Res.* 21, pp. 816.
 14. Sulim I. Y., Borysenko M. V., Korduban O. M. and Gun'ko V. M. (2009). *Appl. Surf. Sci.* 255, pp. 7818
 15. Gun'ko V. M., Sulym I. Y., Borysenko M. V. and Turov V. V. (2013). *Colloids Surf. A: Physicochem. Eng. Aspects* 426, pp. 47.
 16. Truffault L., Magnani M., Hammer P., Santilli C. V. and Pulcinelli S. H. (2015). *Colloids Surf. A: Physicochem. Eng. Aspects* 471, pp. 73.

Corresponding Author

Dr. Shashwati Vijay Pradhan*

Assistant Professor, R. D. National College, Bandra,
West-Mumbai

vshashu@gmail.com